NASA

Technical Memorandum 78111

Numerical and Laboratory Simulation of Fault Motion and Earthquake Occurrence

Steven C. Cohen

APRIL 1978

National Aeronautics and Space Administration

Goddard Space Flight Center
Greenbelt, Maryland 20771

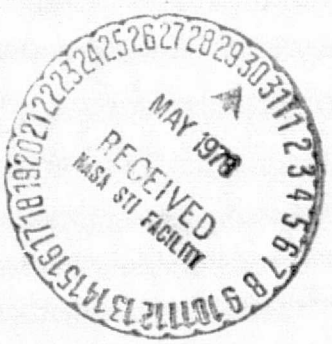

NUMERICAL AND LABORATORY SIMULATION OF FAULT MOTION AND EARTHQUAKE OCCURRENCE

Steven C. Cohen

Geodynamics Branch

Goddard Space Flight Center

Greenbelt, Maryland 20771

April 1978

GODDARD SPACE FLIGHT CENTER

GREENBELT, MARYLAND

NUMERICAL AND LABORATORY SIMULATION OF FAULT MOTION AND EARTHQUAKE OCCURRENCE

Steven C. Cohen

Geodynamics Branch

Goddard Space Flight Center

Greenbelt, Maryland 20771

ABSTRACT

This paper reviews the simulation of earthquake occurrence by numerical and laboratory mechanical block models. Simple linear rheologies are used with elastic forces driving the main events and viscoelastic forces being important for aftershock and creep occurrence. Friction and its dependence on velocity, stress, and displacement also plays a key role in determining how, when, and where fault motion occurs. The discussion of the qualitative behavior of the simulators focuses on the manner in which energy is stored in the system and released by the unstable and stable sliding processes. The numerical results emphasize the statistics of earthquake occurrence and the correlations among source parameters.

CONTENTS

ILLUSTRATIONS

ILLUSTRATIONS (Continued)

TABLE

NUMERICAL AND LABORATORY SIMULATION OF FAULT MOTION AND EARTHQUAKE OCCURRENCE

I. INTRODUCTION

This paper reviews numerical and experimental simulations of fault motion and earthquake occurrence. In the simulations discussed here fault regions are represented by discrete blocks which are driven across a friction surface by various combinations of elastic and viscous force elements. This representation of earthquake sliding and associated fault dynamics has both strengths and weaknesses which can be stated from the outset. Foremost among its strengths are its clarity and conceptual simplicity. The modeling of fault dynamics in terms of sliding blocks is readily accomplished both in the laboratory and on a computer. The details of the sliding process appeal to intuition and experience and thereby permit a clear understanding of the observed behavior. Many of the large scale phenomena associated with earthquakes and fault motion are mimiced in the simulations including the occurrence of foreshocks, main shocks, and aftershocks in single earthquake sequences, the correlation among source parameters such as that between energy drop and the product of rupture length and average displacement, and the occurrence of stable, aseismic, sliding episodes. In addition, the simulation technique provides a convenient test bed for examining new models of earthquake source mechanisms and for exploring

their dynamic consequences. The simplicity of the technique also accounts for its weaknesses. Aside from the obvious dangers of oversimplification of complicated tectonic and geologic processes, the lumpiness of the block elements introduces restrictions of the length scale of the phenomena which can be studied and introduces a discretization which may not be present in nature.

While this review will concentrate on the mechanical block representation of earthquake occurrence, note should be made of the dislocation theory techniques for studying some of the same problems that will be discussed here. Dislocation techniques usually, although not necessarily, assume some known rupture propagation characteristics along the surface expression of a fault and deduce the consequential motions of points elsewhere. Dislocation techniques have been discussed by Haskell (1969) among others.

The organization of this paper is as follows. In the remainder of the introduction we present a simple mathematical analysis of the sliding occurring in an earthquake, the model consisting of a single mass block being driven by elastic loading. This model serves as a basis for the more sophisticated models introduced later. With the basic ideas introduced by this model in mind, we begin in Section II a systematic discussion of simulation concepts. This section discusses linear rheological models of the stress-strain relations in rocks. Particular emphasis is place on the time dependent behavior. Section II also reviews various concepts and experiments concerning the frictional resistance to sliding, particularly stick-slip sliding which appears to be

important in earthquake dynamics. In Section III we discuss in a qualitative manner the behavior of various simulators which use the rheological models discussed in the previous section. Then in Section IV we discuss simulator statistics and correlations among source parameters as deduced from the experiments and calculations. Where possible the results are compared with results for naturally occurring events. In the final two sections we discuss several topics related to simulator analysis, present our conclusions, and comments on the possibilities for future research.

We begin the discussion of earthquake fault motion by considering the model, shown in Figure 1, of a block sitting on a friction surface and subject to stress due to the accumulation of elastic strain within a spring. The spring, with elastic constant k, is stretched at constant velocity u. In the absence of any initial motion in the block (mass=m), the frictional resistance prevents sliding until the stress rises to the maximum frictional strength, f^s. Once sliding has begun, the frictional resistance drops to the dynamic value, f^d. Thus with the initial position of the block at $x = 0$, motion is initiated at time t_0 when

$$kut_0 = f^s \tag{1}$$

and thence

$$m\ddot{x} = k(ut - x) - f^d \tag{2}$$

The solution of equation 2 is

$$x = \frac{2(f^s - f^d)}{k} \sin^2 \sqrt{\frac{k}{m}} \frac{(t - t_0)}{2} + u(t - t_0) - u\sqrt{\frac{m}{k}} \sin \sqrt{\frac{k}{m}} (t - t_0) \quad (3)$$

For practical purposes, once the sliding event is initiated we can ignore terms in u since these terms contribute negligible displacements during the time span of an earthquake (typically u = 5 cm/yr; this approximation is mathematically equivalent to setting $t = t_0$ on the right side of equation 2 which then becomes $m\ddot{x} + kx = f^s - f^d)$. Hence

$$x \approx \frac{2(f^s - f^d)}{k} \sin^2 \sqrt{\frac{k}{m}} \frac{(t - t_0)}{2} \quad (4)$$

From this equation we deduce the following:

a. duration of the event

$$\Delta t = \pi \sqrt{\frac{m}{k}} \quad (5)$$

b. total displacement

$$\Delta x = \frac{2(f^s - f^d)}{k} \quad (6)$$

c. reduction in driving tension, ΔF, or fractional driving tension, $\Delta F/F_0$

$$\Delta F = 2(f^s - f^d); \quad \frac{\Delta F}{F_0} = 2\left(1 - \frac{f^d}{f^s}\right) \quad (7)$$

d. potential energy drop

$$\Delta E = f^d \Delta x = \frac{2}{k} f^d (f^s - f^d) \quad (8)$$

e. peak velocity

$$\dot{x}_{max} = \frac{f^s - f^d}{\sqrt{mk}} \tag{9}$$

f. peak acceleration

$$\ddot{x}_{max} = \frac{f^s - f^d}{m} \tag{10}$$

Notice that the reduction in the driving spring tension is independent of the elastic constant and the block mass; in fact, the mass affects only the duration of the event, the velocity and acceleration. Illustrating the relationships by taking $m = 3 \times 10^{18}$ gm, $k = 1 \times 10^{18}$ dyne/cm, $f^s = 2 \times 10^{20}$ dyne, $f^d = 0.8\, f^s$, (corresponding roughly to a ten kilometer cube at shallow depths)

$$\Delta t = 5 \text{ sec}$$

$$\Delta x = 40 \text{ cm}$$

$$\Delta F = 4 \times 10^{19} \text{ dyne}$$

$$\frac{\Delta F}{F_0} = 0.4$$

$$\Delta E = 3 \times 10^{21} \text{ ergs}$$

$$\dot{x}_{max} = 12 \text{ cm/sec}$$

$$\ddot{x}_{max} = 20 \text{ cm/sec}^2$$

This model of blocking sliding under the influence of spring loading introduces many of the concepts advanced in the more complicated models discussed later. For now, however, we turn to a discussion of the fundamental stress-strain relations for rocks.

II. LINEAR RHEOLOGIC MODELS OF STRESS AND STRAIN IN ROCKS; FRICTION

The modeling of fault motion requires as a fundamental starting point some relationship between the stress, σ, acting on the rocks and the consequential strain, ϵ*. In general these relationships can be quite complicated but considerable understanding can be achieved by restricting the analysis to relationships which are linear, that is those which involve stress, strain, or their time derivatives to only the first power. Mathematically this is an extremely powerful assumption for it permits either the total stress or strain due to several elements to be determined by summing individual contributions. The relationships that we state will be for the case of uniaxial compression, no greater generalization will be required at present. The simplest case, that of pure elasticity is,

$$\sigma = k\epsilon \tag{11}$$

A substance obeying this relationship is said to be linear elastic or Hookean. A linear viscous substance, or Newtonian viscous, is defined by

$$\sigma = \eta\dot{\epsilon} \tag{12}$$

More complicated substances can be constructed from combinations of these elements, and the very powerful linear operator techniques can be used to derive the stress-strain relations. We write an element stress-strain relation

*In accordance with common practice we will often mix the concepts of force and stress. In the present context the difference between the tensor nature of stress and the vector nature of force is not of great significance.

as

$$\sigma = O\dot{\epsilon} \tag{13}$$

where O is a linear operator on $\dot{\epsilon}$. For the elastic element $O\dot{\epsilon} = k\int\dot{\epsilon}dt \equiv kI\dot{\epsilon} = k\epsilon$, while for the viscous element $O\dot{\epsilon} = \eta\dot{\epsilon}$. In formal manipulations the inverse of the integration operator is the differentiation operator; i. e., $ID = DI = 1$. For elements connected in series as in Figure 2a, the strains, and hence the strain rates, add directly, i.e., $\dot{\epsilon} = \dot{\epsilon}_k + \dot{\epsilon}_\eta$ or

$$\dot{\epsilon} = [(kI)^{-1} + \eta^{-1}]\,\sigma \tag{14a}$$

Hence

$$\dot{\sigma} + \frac{k}{\eta}\sigma = k\dot{\epsilon} \tag{14b}$$

This is the stress-strain relation for the Maxwell viscous substance formed from the series combination of Hookean and Newtonian elements. As shown in Figure 3, the strain increases linearly with time when the stress is held constant in such a substance. The stress decreases exponentially with time constant $\tau = \eta/k$ when the strain is held constant.

When elements are connected in parallel as in Figure 2b the stresses add directly. Thus for this so called Kelvin element

$$\sigma = \eta\dot{\epsilon} + k\epsilon \tag{15}$$

In contrast to the behavior of the Maxwell substance, the Kelvin substance under

constant stress obeys the relation

$$\epsilon_0 = \epsilon_0 e^{-t/\tau} + \frac{\sigma}{k}(1 - e^{-t/\tau});\ \tau = \frac{\eta}{k} \tag{16}$$

Thus in the absence of any stress the initial strain relaxes exponentially while, if the substance is initially unstrained, the strain rises toward an asympotic value σ/k (Figure 3). When the strain is held constant the stress is the same as that for the linear elastic element. The Kelvin element is the simplest model to give transient creep shown, for example, by the time dependent terms in Equation 16 (Jaeger and Cook, 1976). It is not adequate however for representing seismic activity because it does not permit instantaneous elastic strain (Jaeger and Cook, 1976).

There are two non-degenerate three element substances. These are shown in Figure 2c and 2d. It should be noted that there are alternative equivalent representations of these models. For example, Figure 2c can be replaced by a spring, k_1, in parallel with a series combination of a spring, k_2, and a dashpot (viscous element) η, provided

$$k_1 = \frac{k_a k_b}{k_a + k_b}\ ,\quad k_2 = \frac{k_a^2}{k_a + k_b}\ ,\quad \eta = \left(\frac{k_a}{k_a + k_b}\right)^2 \eta'$$

The stress-strain relationship for the generalized Kelvin substance is

$$\dot{\sigma} + \frac{k_a + k_b}{\eta'}\sigma = k_a \dot{\epsilon} + \frac{k_a k_b}{\eta'}\epsilon \tag{17}$$

Thus under conditions of constant stress

$$\epsilon = \epsilon_0 e^{-t/\tau} + \left(\frac{1}{k_a} + \frac{1}{k_b}\right)\sigma(1 - e^{-t/\tau}); \quad \tau = \frac{\eta'}{k_b} \tag{18}$$

and under constant strain

$$\sigma = \sigma_0 e^{-t/\tau'} + \frac{\epsilon}{\frac{1}{k_a} + \frac{1}{k_b}} (1 - e^{-t/\tau'}); \quad \tau' = \frac{\eta'}{k_a + k_b} \tag{19}$$

Examining equations 18 and 19 we see that this substance shows transient creep and transient stress although for $t \gg \tau, \tau'$ both the stress and strain approach steady state values (Figure 3). Instantaneous stress and strain changes are also possible. Thus this model is useful in discussing transient creep and time dependent stress readjustment following major sliding events. These features will prove to be important in modeling aseismic fault motion and aftershocks.

For the other non-degenerate three element substance

$$\dot{\sigma} + \frac{k}{\eta_a + \eta_b} \sigma = \frac{\eta_a \eta_b}{\eta_a + \eta_b} \ddot{\epsilon} + \frac{\eta_a k}{\eta_a + \eta_b} \dot{\epsilon} \tag{20}$$

Thus for constant stress

$$\epsilon = \epsilon_0 + \frac{\sigma t}{\eta_a} + \left(\dot{\epsilon}_0 - \frac{\sigma}{\eta_a}\right)\tau(1 - e^{-t/\tau}); \quad \tau = \frac{\eta_b}{k} \tag{21}$$

and for constant strain

$$\sigma = \sigma_0 e^{-t/\tau}; \quad \tau = \frac{\eta_a + \eta_b}{k} \tag{22}$$

which has the same form as the Maxwell substance under constant strain.

Four element models can also be used to simulate features of fault dynamics. Figure 2e shows one form, the Burgers substance, which consists of a series combination of Kelvin and Maxwell elements. The stress-strain relation is

$$\ddot{\sigma} + \left[\frac{k_a}{\eta_a} + \frac{k_b}{\eta_b} + \frac{k_a}{\eta_b}\right]\dot{\sigma} + \frac{k_a k_b}{\eta_a \eta_b}\,\sigma = k_a \ddot{\epsilon} + k_a \frac{k_b}{\eta_b}\,\dot{\epsilon} \qquad (23)$$

This model shows instantaneous strain and both transient and steady state creep but because of its complexity has not been used in a detailed simulation of the type currently under discussion.

The linear operators we have used here are directly analagous to those appearing in other fields, particularly electrical circuit theory. The equation $\sigma = O\dot{\epsilon}$ is analagous to the electrical equation $J = \sigma E$ where J is the electric current density and E is the electric field amplitude. Thus stress is analagous to current density and strain is analagous to the electric field amplitude. The operator O is analagous to conductivity or the electrical admittance. Its inverse is resistivity or impedance. Thus the viscous element with a direct proportionality between σ and $\dot{\epsilon}$ plays the role of a resistor, and the spring that of an inductive coil. It can also be shown that the inertial effect of the block mass, m, is analogous to the capacitive effects in electrical circuits.

In the preceeding discussion we have developed equations relating stress and strain for a number of model substances. If the mechanical block discussed in Section I were free to move without encountering frictional resistance then it would undergo a continual slow movement to prevent any long term

stress accumulation. This would not, however, be an adequate model of fault surfaces where frictional interactions between the opposite sides of the fault act to restrict motion. Thus we need to include in the simulator a description of the frictional properties of rocks in the fault zone. We again consider a block model with the block resting on a surface and subject to a compressive normal stress, σ. When a shear stress is applied parallel to the contact plane, it is found that over a wide range of normal stresses and temperatures and for a wide range of rock materials, that no motion occurs until some critical magnitude of shear stress, F^s, is reached. An experimental relationship between F^s and σ can be deduced viz,

$$F^s = \mu^s \sigma \tag{24}$$

where μ^s is the coefficient of static friction. Experiments have found that to a good approximation μ^s is only a weak function of the area of contact and the normal stress (Jaeger and Cook, 1976). Once sliding is initiated, it is again observed that the frictional resistance is proportional to normal stress but, as a general rule, the proportionality constant, μ^d, known as the dynamic friction coefficient is less than the static coefficient. The value of the dynamic friction coefficient may vary with the speed of sliding.

When careful measurements are made of the relationship between static friction and normal stress it is found that the F^s versus σ curve does not pass through the origin, but that to a better approximation $F^s = F_0 + \mu\sigma$ where F_0 corresponds to an intrinsic shear strength.

We also have not yet considered a possible time dependence of fric-

tion. In general one might expect that the static friction coefficient will increase with the duration of contact following some earlier sliding, corresponding to a time dependent healing of the ruptured region. Dieterich (1972a) has observed this effect and concludes

$$\mu^s(t) = \mu^s(0)\,[1 + \alpha \log(\Delta t)]\,;\, \Delta t > 1 \text{ sec.} \qquad (25)$$

where Δt is the duration of contact following sliding.

A different approach to the frictional resistance in block sliding has been discussed by Byerlee (1970), Nur and Shultz (1973), and Nur (1977) in light of earthquake dynamics. In this approach it is assumed that asperities along the fault surface lock together to form the frictional resistance. When the shear force becomes strong enough to cause brittle failure of these asperities motion can occur. As the sliding proceeds, continual locking and breaking of the asperities cause fluctuations in the frictional resistance. Thus, the frictional resistance varies in some irregular manner with displacement. In this model the value of the frictional resistance at the initiation of the unstable sliding event is analogous to the static friction and the average value of the fluctuating friction during the earthquake sliding corresponds to the dynamic friction. An interesting feature of this model is that both rapid, unstable sliding resembling that occuring in earthquakes and slow, stable sliding resembling that in creep events can occur. The criterion for unstable sliding is that the driving stress decease less rapidly with displacement than the frictional resistance.

In the earthquake simulations, various models for the frictional resistance will be employed. In the simplest cases, static and dynamic friction forces, f^s

and f^d, are used to explain the gross features of the main sliding events. Other models are introduced for modeling aftershocks, creep, and the details of the earthquake instability mechanisms.

III. MODEL SIMULATIONS - GENERAL RESULTS

The prototype for the models that are discussed in this paper is shown in Figure 4. It consists of a number of masses connected together by springs and resting on a friction surface. The masses are driven by springs connected to a moving plate. In some early laboratory simulations only the first mass of the chain was connected to a driving source. In many of the computational models the springs have been replaced by more complicated rheological elements such as the viscoelastic elements discussed in the previous section. Details concerning the various laboratory and computational models that are discussed in this review can be found in the Appendix.

The simplest models of fault motion during earthquakes employ elastic springs as coupling elements and frictional surfaces over which the blocks slide. Laboratory models of this type have been studied by Burridge and Knopoff (1967), King and Knopoff (1968b), and King (1975). Computational models include those of Dieterich (1972b, 1973), Otsuka (1972a), Cohen (1977a, 1977b), and Rundle and Jackson (1977). In examining the sequence of events occurring in their simulator, Burridge and Knopoff (1967) found that small events occur largely at random while large events involving major changes in elastic potential energy occur nearly periodically. Between major events the potential energy of the system increased nearly linearly with time when the inter-

mass springs had equal elastic constants. Furthermore, the major events all occurred at approximately the same level of potential energy and involved comparable energy drops. Thus the period between these large events was simply the energy drop divided by the rate of energy input.

King and Knopoff (1968b) also found in their study that the strain energy density before a shock showed little variation with the magnitude of the event. An analagous result has been reported by Bath and Duda (1964) for natural events. King (1975) observed a long term linear trend in average displacement with time; this behavior is, of course, necessary since in the long term the displacement rate must keep pace with velocity of the moving splate. More significantly, he noted that large shocks occurred at times when the displacements of most masses had fallen below their long term averages. On the other hand King, unlike Burridge and Knopoff (1967), reported that large shocks were not periodic in time.

Using a computational model in which friction was allowed to vary from block to block, Dieterich (1972b) found that the frequency with which blocks move is related to their static frictional strength with low friction blocks moving more frequently than those with high friction. * Dieterich (1973) also performed two and three dimensional simulations and derived scaling laws that relate source parameters obtained with one set of input variables to source parameters with a new set of input parameters. These important scaling laws are summarized in Table I.

*One contrast between the laboratory and computational models should be noted. In the laboratory model, stick-slip sliding is observed but there is no certainty about the mathematical description of the friction law. In the computational model the friction law is clearly defined mathematically, but it is not certain how well the mathematical description represents the natural process.

The importance of seismic gaps, that is regions of low seismic activity in an otherwise highly seismic region, has long been studied for earthquake prediction purposes. Otsuka (1972) found that large simulation earthquakes occurred in regions of anomalously low seismic activity.

Studies have also been performed to determine how the qualitative characteristics of fault movements are influenced by the degree of heterogeneity in the friction and elastic parameters. Cohen (1977b) has found, for example, that with relatively homogeneous fault parameters successive events tend to propagate along the length of the fault in a type of epicenter migration. He also found that recurrence patterns in the locations and magnitudes of seismic activity could be observed. Both effects were less common with heterogeneous faults, but seismic gaps were more likely to occur.

Rundle and Jackson (1977) searched for evidence of an increase in simulator seismicity preceeding large events such as suggested by studies of California seismicity by Wesson and Ellsworth (1973) and Wyss and Lee (1973). Such behavior was not present in their elastic model leading them to speculate that the seismicity increases may be due to (among other causes) time dependent fault parameters.

Several workers, including Rundle and Jackson (1977) have pointed out that as the ratio of elastic modulus to stress increases, there are frequent small displacements and the system behavior becomes ductile. Conversely as the ratio decreases larger infrequent events occur.

In the models that have been discussed up to now the only significant time dependent processes have been the slow elastic loading of the driving springs and the sudden elastic motions during simulation earthquakes. As a consequence the models are not capable of explaining phenomena occuring on intermediate time scales. The most important of these intermediate scale phenomena are earthquake sequences involving either foreshocks, the main shock, and aftershocks or nearly equal magnitude swarms. Other important time dependent phenomena include continuous, episodic, premonitory, and post seismic creep. To study some of these effects, various computational models of viscoelasticity and time and stress dependent friction have been employed. In the earliest of these models Burridge and Knopoff (1967) divided their one dimensional fault into three regions, two regions with predominately elastic properties and low viscosity separated by a region of high viscosity. The effect of the viscous region was to introduce a time delay between the time of sliding in one elastic region and the time at which the resultant stress change was felt in the other elastic region. This time delay was responsible for the occurrence of aftershocks both in the secondary and in the primary elastic regions. In the high viscosity region, unstable sliding could not occur. The time dependent characteristics of the energy release in the viscoelastic model were significantly different from the elastic case. In a sequence of 69 aftershocks following a main shock on the primary fault, the authors reported:

1. The cumulative energy released by aftershocks increased as $(1 - e^{-t/\eta})$.

2. The total stress energy released in the shock sequence was divided as follows: main shock - 12%, aftershocks on primary segment - 44%, aftershocks on secondary segment - 13%. Additionally a potential energy release equal to 43% of the energy released by simulation shocks was dissipated by viscous flow.

3. Despite the greater energy release in the primary segment, only 27% of the shocks, including the main shock, occurred along this segment.

4. The decay in the frequency of aftershocks occurring with time was fairly consistent with either the $(1 + \beta t)^{-1}$ dependence suggested by Omori (1894) or an exponential decay.

It may be significant to note that in this sequence more potential energy is released by aftershocks than by the main shock. We will comment more on this point later.

Dieterich (1972b) has proposed that the interplay of viscoelastic stress recovery following an earthquake coupled with a reduced frictional strength of the fault following a sudden sliding may be responsible for aftershocks. Consider the generalized Kelvin substance discussed in section II.. It can be shown that following a sudden stress relaxing sliding event, a time dependent increase in stress can occur with the stress rise asymptotically approaching $k_a / (k_a + k_b)$ of the stress drop during the sliding. Furthermore, as Dieterich's (1972a) experimental work suggests, the frictional resistance against further sliding

is less than the resistance prior to sliding. Presumably this is related to the finite time required for frictional healing of the rupture (equation 25). If the viscoelastic stress recovery is more rapid than the time required for fault healing an aftershock may be generated. The aftershocks occur in the same region of the fault that ruptured during the original event and the duration of the aftershock sequence increases with the size of the main shock. Furthermore a correlation has been found between the dispacements and magnitudes in the main shock and those of the largest aftershock's (Cohen, 1977b). Although the frequency of aftershocks decreases with time, it does not follow Omori's law (Dieterich, 1974).

In an alternative model of aftershocks, Rundle and Jackson (1977) focused attention on stress induced crack nucleation. They assumed that the friction strength, F^s, against sliding decreases at a rate proportional to the amount the stress exceeds some value of friction, F^{su}, i.e.,

$$\frac{dF^s(t)}{dt} = -\frac{1}{\tau}[\sigma(t) - F^{su}] \tag{26}$$

where F^{su} is a constant and $\sigma(t)$ is the stress acting on the block. In this model, if the dynamic friction is greater than F^{su}, the stress drop during the first rupture is small and the stress, $\sigma(t)$, remains large causing a decrease in frictional strength. Since friction is then reduced while stress remains high aftershocks may occur. The aftershocks are not confined to the region of the primary shock since a stress induced failure may also occur in a region

adjacent to that which ruptured during the primary event (this border region having been stressed by the elastic elements coupling it to the displaced region). Since the stress, $\sigma(t)$, generally changes little on the time scale of τ, τ is also the time scale for the aftershock occurrence. Rundle and Jackson's results show too few aftershocks to examine the dependence of aftershock frequency on time following the main shock, however, it may be necessary to introduce some time variation in $\sigma(t)$, other than the tectonic loading rate, to produce a decaying frequency of aftershocks resembling that present in nature.

IV. STATISTICS, SOURCE PARAMETERS, AND CORRELATIONS

Up to this point our discussion of simulator results has been primarily descriptive. Quantitative results generally fall into two categories - one, the statistics of earthquake occurrence and two, the correlations among source parameters. Considering first the frequency of simulator earthquake occurrence as a function of the energy released in the events Burridge and Knopoff (1967) obtained the experimental results shown in Figure 5. Except for the lowest energies the data fit a straight line with

$$\log f = A - B \log E \tag{27}$$

where f is the frequency of events occurring with energy greater than or equal to E. This relationship appears analagous to the relationship between the frequency of naturally occurring events and the seismic energy $\log f = A' - B' \log E_s$. Bearing in mind the relationship between seismic energy and earthquake

magnitude, viz, $\log E_s = a + bM$ it is tempting to define a magnitude for the simulator events by

$$M_{SIM} = \log E \tag{28}$$

This analogy suggests a linear relationship between log E and log E_s and while this is a useful viewpoint it is only an approximation whose validity needs to be confirmed. A reason for the flattening of the simulator frequency versus magnitude curve at low magnitudes is that the discrete nature of the model imposes some lowest magnitude event below which no events will occur.

For naturally occurring events $B' = 0.4$ while Burridge and Knopoff (1967) found $B = 1$ in their mechanical simulator. These authors have conjectured that the difference between their simulator results and actual earthquake data may be a reflection of the one-dimensional nature of their model. However for a very similar mechanical model, King and Knopoff (1968) found $B = 0.71$ and for a later laboratory model King (1975) found $B = 0.5$. Rundle and Jackson (1971) concluded that the results from their computational simulator could be fit to two lines with $B = 0.1 - 0.5$ for low magnitude events and $B = 1$-5 for high magnitude events. An alternative analysis by Otsuka (1972b) revealed downward curvature in the logarithm of frequency versus magnitude curve, the degree of downward curvature decreasing with the probability that the motion of one blocks stimulates an adjacent block into motion. A similar curvature was found in the computational simulator by Cohen (1977a). Although it appears that there is

some qualitative agreement between the deviations from a linear behavior for some actual earthquake data and the numerical results, the quantitative agreement is at best only fair.

The variation in the frequency of the time intervals between events can be examined to determine whether the distribution of interevent periods is Poissionian as would be expected if the events occur randomly in time. Both Burridge and Knopoff (1967) and Rundle and Jackson (1977) have found some non-Poissonian components to the distribution, presumably due to the interactions between adjacent events. The motion of one block alters the stretch or compression of the spring connecting it to the neighboring block thus altering the stress and the time at which the stress overcomes the frictional resistance. However, Knopoff, Mitchel, and Jackson (1972) and Rundle and Jackson (1977) have shown that the occurrence rate for the simulation events are consistent with a stochastic model operating on the stored elastic energy. They have used in their analyses the Kolmogorov backward equation

$$\lambda(E)P(E) + \alpha \frac{dP(E)}{dE} = \int_0^{E_{max}-E} T(E,x)\lambda(x)P(x)\,dx \qquad (29)$$

where now E is the elastic potential energy of the system, $\lambda(E)$ is the probability that an event will occur in time interval dt if the energy is E, α is the rate at which energy accumulates between events, $T(E,x)\,dE$ is the probability that if an event occurs at initial energy the final energy will be in the range E to $E + dE$ and $P(E)dE$ is the probability of finding the system energy between

E and E + dE. Figure 6 shows the degree with which the Kolmogorov equation fits the results of Rundle and Jackson (1977).

King and Knopoff (1968b) used their mechanical simulator to deduce correlations among the rupture parameters for model shocks. Shock energy is shown in Figure 7 as a function of the length of tne rupture, ℓ, or the number of displaced masses, L. The data shows a concave up behavior on the log-log plot of Figure 7; however, if the data with L = 8 are excluded a linear correlation with log E = 1.3 + 1.6 log L can be used. Since L = 8 corresponds to movement within the entire spring-mass system and since the free boundary conditions of the end masses are not representative of natural conditions, the data with N = 8 must be viewed with caution. Dieterich (1974) has assembled a number of magnitude versus rupture length relations used by various workers. In general they have the form m = g + h log ℓ with h between one and two.

Somewhat better linear correlations are discovered when log E is plotted against log LD, log LD^2, and log Ld where D and d are the peak and average displacements of the blocks. The correlation between E and Ld is shown in Figure 8. The relationship $E \propto \ell d$ will be established below while the relation $E \propto \ell D^2$ (or $E \propto \ell d^2$) has been deduced from calculations based on an electrostatic analog (Knopoff, 1958). In a study of earthquake data King and Knopoff (1968a) deduced

$$\log \ell D^2 = 2.24M - 4.99 \tag{30a}$$

while in their simulator work (King and Knopoff, 1968b) they found

$$\log LD^2 = 1.55 \log \frac{2B}{k} - 1.89 \tag{30b}$$

Assuming $\log E_s = 11.8 + 1.5M$ and $E \approx \eta E_s$ where η is the seismic efficiency, the simulator results give

$$\log LD^2 = 2.3M + 1.64 + 1.55 \log \frac{2}{\eta K} \tag{30c}$$

Thus the slopes of the curves of $\log LD^2$ versus M are comparable for the natural and simulated events provided the assumed relationship between seismic energy and simulator energy is valid.

Some of the results presented in the preceeding paragraph can be explained by relatively simple theoretical arguments. For simulations in which the elastic energy stored in the driving and connecting springs is dissipated by friction sliding, the energy drop during an event is

$$E = \sum_i f_i^d \Delta x_i \tag{31}$$

where the sum is taken over the blocks that move in the event. We consider two cases. If only one block moves, then with reference to Figure 4

$$\Delta x = D = d = \frac{2(f^s - f^d)}{k_i + k_{i+1} + k_i^g} \tag{32}$$

From this we can deduce that $E \propto \mathcal{L}D^2$; here $\mathcal{L}$ is the dimension of the block. This result agrees with the aforementioned result by Knopoff (1968). In the second case we assume the friction varies little from block to block so

it can be removed from under the summation sign and

$$E = f^d \sum_i \Delta x_i = f^d L d \tag{33}$$

a result agreeing with the correlation suggested by Figure 8.

The preceeding analysis can also be used to explain the simulation observed variation in average displacement versus magnitude. From equation 33 we deduce

$$d = \frac{E}{f^d L} \propto \frac{10^{M_{SIM}}}{L} \qquad f^d = \text{constant} \tag{34}$$

Alternatively for single block motion

$$d \propto \sqrt{\frac{E}{\mathcal{L}}} \propto \frac{10^{M_{SIM}/2}}{\sqrt{\mathcal{L}}} \qquad \text{one block} \tag{35}$$

The simulation data shown in figure 9 are consistent with these equations.

The change in the elastic force in the spring-mass systems due to the unstable sliding in an event is simply

$$\Delta F = \sum_i k_i^{\ell} \Delta x_i \tag{36}$$

or if the driving spring moduli are all approximately equal

$$\Delta F = k^{\ell} L d \tag{37}$$

Thus in the case where both equations 34 and 37 are valid $\Delta F \propto \Delta E = 10^{M_{SIM}}$ while for single block motion $\Delta F \propto 10^{M_{SIM}/2}$. One observed variation in the stress drop in the driving springs versus log E is shown in Figure 10. In general the data

for $L < 8$ suggest that while the stress drop increases with magnitude it does so more slowly than indicated by the preceeding equations.

Different simulations have indicated somewhat different variation in displacement with rupture length. Results obtained by both King and Knopoff (1968b) and King (1975) revealed both increasing average and peak displacement with increasing rupture length. By contrast Cohen (1977b) discovered that the average displacement increased with rupture length for small numbers of displaced blocks but for longer ruptures found no further increase in average displacement. Wallace (1974) has assembled data relating rupture length and maximum displacement to earthquake magnitude for earthquakes in Western North America. His data indicates that maximum displacement increases about linearly with rupture length although there is considerable data scatter. These results agree better with those of King (1975) and King and Knopoff (1968b), than those of Cohen (1977b).

V. OBSERVATION AND DISCUSSION OF RELATED TOPICS

It is interesting to consider for a moment the mathematical origin of the instability that characterizes the sliding process in various simulations. In the simplest models, the instability is due to the sudden transition from the static to the lower dynamic friction when the driving force equals the static friction. Burridge and Knopoff (1967) used a more complicated friction law and deduced that the condition for instability on a single block is that the net friction force decrease with increasing velocity at the beginning of unstable sliding.

(A similar friction law which is mathematically smoother than that of Burridge and Knopoff but which reduces to their law in the limits of small and large velocities has been used by Whithead and Gans (1974)). Thus the simple model is contained within the more general treatment of Burridge and Knopoff. Notice that the instability condition focuses on the variation in stress for a change in velocity. A somewhat different view advanced by Nur and coworkers and alluded to in Section II, focuses on how the stress changes with displacement. If $F(x)$ is the net driving force and $f(x)$ a position dependent friction then the condition for unstable sliding in a region of decreasing friction is $-f'(x) > -F'(x)$. For the purely elastic case in which $F(x) = k(ut - x)$, this condition is $-f'(x) > k$. This instability condition implies, in the elastic case, that friction decrease more rapidly with displacement than the reduction in the elastic spring driving tension. The most detailed quantitive calculation in Nur's so called stiffness model has been performed with a one block viscoelastic substance (Cohen, 1978). The most interesting features that emerge are

1. creep occurs premonitory to unstable sliding episodes. Transient creep may also occur after unstable sliding.
2. stable sliding occurs on both epidsoic and long-term time time scales. Episodic sliding events may be stable or unstable depending on the interplay between the viscoelastic and friction parameters.

Despite these apparent correlations between the viscoelastic stiffness model and naturally occurring events, it must be emphasized that there is

considerable uncertainty about the basic validity of the stiffness theory. Model calculations can only deduce the consequences of the assumptions and it can happen that alternative assumptions have the same consequences.

Knopoff (1972) advanced a theory of aftershock occurrence which contains some of the elements of other aftershock models and in a sense anticipated some of the later developments. The two key elements in Knopoff's model are the occurrence of large stresses on the edges of a rupture zone of a shock and the delay in rupture of a highly stressed region by prerupture tertiary creep. In application Knopoff notes that because of the elastic properties the boundary between a region that slid during an earthquake and the neighboring unmoved region is one of high stress concentration. Knopoff, like Rundle and Jackson (1977), postulated that this highly stressed boundary region may not fail instantaneously but may fail with a delay time dependent on the degree of overstressing. This delayed response gives rise to aftershocks which cluster around the edges of the main shock rupture region. As already noted failure, in this model, occurs with preshock tertiary creep.

A common feature of the viscoelastic aftershock theories that we have reviewed in this paper is the occurrence of either creep or stress recovery following the primary shock. The fundamental study of the relationship between aftershocks and creep using the linear circuit theory that we presented in Section II is due to Benioff (1951). In applying his theory to a number of earthquake sequences Benioff concluded that while the seismic wave energy of the primary

shock exceeds that of the entire aftershock sequence, the elastic strain energy dissipated in the creep-aftershock sequence may be comparable to that of the primary shock. In the earlier discussion of the numerical model of Burridge and Knopoff (1967) we pointed out that more potential energy was released in the aftershock and creeping following the main shock than was released in the main shock. These two results strongly suggest that aftershocks and post-seimic creep may be responsible for a much larger fraction of the total elastic energy dissipation than would be suggested by their seismic wave magnitudes.

As we mentioned earlier the spring and block models that have been reviewed in this paper are just a small subset of all models of fault motion and earthquake occurrence. As one alternative approach rock mechanics experiments involving the sliding of small rock samples have provided a wealth of data on the rupture and sliding processes. In the last several years Brune (1973) has used stressed foam rubber to observe both stick slip sliding and creep. Along computational lines, dislocation theory has been used to determine ground displacements, velocities, and accelerations due to fault motions. The models discussed here and dislocation theory models become somewhat similar in concept when the present models are expanded to two and three dimensions and the elements made small, and when the dislocation models are formulated with a description of the rupture process.

VI. CONCLUSIONS

It has been somewhat over a decade since the first massive block simulator of earthquake occurrence was developed. In that time well over a dozen studies have been made by almost as many researchers. Major contributions have been made in understanding the propagation of rupture along a fault, in developing correlations among source parameters, and in explaining the interplay between foreshocks, main shocks, and aftershocks and creep. It appears to the author that at least two areas of study have potential for contributing significant new information. The first of these is the study of two and three dimensional visco-elastic systems, possibly with multiple faults. It seems likely that the interaction of elements not directly on the fault surface will produce a number of effects such as a propagating creep wave not observed in most one dimensional simulations. The second area is the study of the physics connecting the near field block sliding with the far field seismic wave motion. A synthesis of techniques such as a combination of a sliding block description of rupture with a dislocation theory description of the far field effects might prove fruitful. By contrast it seems less likely that fundamentally new insights will be achieved by utilizing more complicated rheological models (although simple, but novel models may be illuminating). The more complicated the rheological model, the greater the number of adjustable parameters that impact the calculations. Thus entirely different models may produce similar effects if the parameters are appropriately adjusted. In this case, the validity of one model as opposed

to another cannot be established. Finally it seems increasingly evident that a detailed understanding of earthquake occurrence will require improvements in the present knowledge of friction laws, rupture criteria, and the physics of highly stressed rock.

REFERENCES

Bath, M., and S. J. Duda, "Earthquake Volume Fault Plane Area, Seismic Energy, Strain, Deformation and Related Quantities, Annali di Geofisica, 17, 353-368, 1964.

Benioff, H., "Earthquakes and Rock Creep, Part I," Bull. Seism. Soc. Am., 41, 31-62, 1951.

Brune, J. N., "Earthquake Modeling by Stick-Slip Along Precut Surfaces in Stressed Foam Rubber," Bull. Seism. Soc. Am., 63, 2105-2119, 1973

Burridge, R., and L. Knopoff, "Model and Theoretical Seismicity," Bull. Seism. Soc. Am., 57, 341-371, 1967.

Byerlee, "The Mechanics of Stick-Slip," Tectonophysics, 9, 475-486, 1970

Cohen, S. C. "Faulting Parameters Derived from Computer Simulation of Earthquakes," X-921-77-142, Goddard Space Flight Center, 1977a.

Cohen, S. C., "Computer Simulation of Earthquakes," J. Geophys. Res., 82, 3781-3796, 1977b.

Cohen, S. C., "The Viscoelastic Stiffness Model of Seismicity," to be published, 1978.

Dieterich, J. H., "Time-dependent Friction in Rocks," J. Geophys. Res., 77, 3690-3697, 1972a.

Dieterich, J. H., "Time-Dependent Friction as a Possible Mechanism for Aftershocks," J. Geophys. Res., 77, 3771-3781, 1972b.

Dieterich, J. H., "A Deterministic Near-Field Source Model," Proc. Fifth World Conf. on Earthquake Eng., Rome, 1973.

Dieterich, J. H., "Earthquake Mechanisms and Modeling," Annual Reviews Earth Space Science 275-301, 1977.

Haskell, N. A., "Elastic Displacements in the Near Field of a Propagating Fault," Bull. Seism. Soc. Am., 59, 865-908, 1969.

Jaeger, J. C., and N. G. W. Cook, Fundamentals of Rock Mechanics, pp. 305-322, Halsted, London, 1976.

King, C. Y., and L. Knopoff, "Stress Drop in Earthquakes," Bull Seism. Soc. Am., 58, 249-257, 1968a.

King, C. Y., and L. Knopoff, "Model Seismicity: Rupture Parameters, Stress, and Energy Relations." J. Geophys. Res., 73, 1399-1406, 1968b.

King, C. Y., "Model Seismicity and Rupture Parameters," Bull. Seism. Soc. Am., 65, 245-259, 1975.

Knopoff, L., "Energy Release in Earthquakes," Geophys J., 1, 44-55, 1958.

Knopoff, L., "Model for Aftershock Occurrence," Flow and Fracture of Rocks, AGU geophys. Mono. 16, 1972.

Knopoff, L., R. Mitchel, and D. D. Jackson, "A Stochastic Analysis of a Model Earthquake Sequence," Geophys. J., 29, 255-261, 1972.

Nur, A., and P. Schultz, "Fluid Flow and Faulting 2: A Stiffness Model for Seismicity," Proc. Conf. Tectonic Prob. San Andreas Fault System, Stanford, 1973

Nur, A., "Non-Uniform Friction as a Physical Basis for Earthquake Mechanics," Proc. Conf. II Exp. Stud. Rock Frict. Appl. Earthquake Pred., Menlo Park, 1977.

Omori, F., "On the Aftershocks of Earthquakes," J. Coll. Sci. Imp. Univ. Tokyo, 7, 111-200, 1894.

Otsuka, M. "A Simulation of Earthquake Occurrence," Phys. Earth Planet. Interiors, 6, 311-315, 1972a.

Otsuka, M., "A Chain-Reaction-Type Source Model as a Tool to Interpret the Magnitude Frequency Relation of Earthquakes," J. Phys. Earth, 20, 35-45, 1972b.

Rundle, J. B., and D. D. Jackson, "Numerical Simulation of Earthquake Sequences," Bull. Seism. Soc. Am., 67, 1363-1377, 1977.

Wallace, R. E., "Earthquake Recurrence Intervals on the San Andreas Fault." Geol. Soc. Am. Bull, 81, 2875-2890, 1970.

Wesson, R. L., and W. L. Ellsworth, "Seismicity Proceeding Moderate Earthquakes in California," J. Geophys. Res., 78, 8527-8546, 1973.

Whitehead, J. A., and R. F. Gans, "A New Theoretically Tractable Earthquake Model," Geophys. J., 39, 11-28, 1974.

Wyss, M., and W. H. K. Lee, "The Variations of the Average Earthquake Magnitude in Central California," Proc. Conf. Tectonic Prob. San Andreas Fault System, Stanford, 1973.

Yamashita, T., "On the Dynamical Processes of Fault Motion in the Presence of Friction and Inhomogeneous Initial Stress Part I. Rupture Propagation," J. Phys. Earth., 24, 417-444, 1976.

APPENDIX

The various laboratory and numerical simulations discussed in this paper are summarized below.

1. Burridge and Knopoff (1967)

   a. laboratory model

      One dimensional – 8 masses connecting by springs and driven by stretching of spring connected to first mass; m = 142 gms; spring constant = 2×10^5 dynes/strain; spring lengths: 3 cm or 1.5 - 12 cm; loading rate: 2 cm/sec.

   b. computational model

      One dimensional – 10 masses connected by springs and driven by springs coupling to a moving plate. 5 blocks represent a primary fault, and 3 blocks represent an auxiliary fault. The primary and auxiliary fault segments are separated by two blocks in a highly viscous region. In a normalized system of units m = 1, connecting spring constants = 100, driving spring constants 1, intermass spacing = 1. The friction law is

$$f(\dot{x}) = \begin{cases} -\left(\frac{B}{H} + E\right)\dot{x} & |\dot{x}| < H \\ -\frac{B}{1 + A(\dot{x} - H)} - E\dot{x} & \dot{x} > H \\ \frac{B}{1 - A(\dot{x} + H)} - E\dot{x} & \dot{x} < -H \end{cases}$$

with A = 10, E = 1 (all blocks); H = 10^{-9} (1-3, 6-10), 10^{3} (4, 5) B = 5 (1-3), 10^{9} (4, 5), 15(6), 10 (7-10), when the numbers in parentheses are the block numbers for which the quoted values are applicable. The driving rate in this system of units is 10^{-8} .

2. Kings and Knopoff (1968b)

Laboratory model similar to that used by Burridge and Knopoff (1967); 8 masses: m = 130 gms; spring constants = 10^{5} dynes/cm; spring unstretched length = 3 cm.

3. Otsuka (1972)

Two dimensional computational model; blocks suspended to fixed overhead support by leaf springs and in contact with moving floor. 2000 blocks in a 100 × 20 grid.

4. Dieterich (1972b)

One dimensional computational model; 50 blocks interconnected and driven by coupling to moving plate. Four models are employed in which the coupling elements and the friction vary as follows:

a. elastic springs, time independent static friction

b. elastic springs, time dependent friction

c. viscoelastic elements, time independent friction

d. viscoelastic elements, time dependent friction.

The viscoelastic coupling element is the generalized Kelvin element. The time dependent friction is represented as $f^{s}(t) = f^{s}(t_0)\ [1 + A \log t]$ for $t > 1$ sec.

The numerical values used in the model calculation are: friction stress ~ 100-300 bars, $k_2/k_1 = 1.5 - 5.0$, $\tau = 10^2 - 10^4$ sec, $f^d = 0.8 f^s$ for time independent friction, $f^d = 0.98\ f^s\ (t_0)$ for time dependent friction, A = 0.02, interelement spacing = 1 km, driving plate velocity = 5 cm/yr

5. Dieterich (1973)

Two and three dimensional computational models in which the boundary conditions are specified displacements of blocks far removed from the fault. Elastic springs are assumed, length to width ratio of the region varies from 2-4.

6. King (1975)

One dimensional laboratory model in which masses are driven by coupling to an overhead rotating flat circular plate; 8 masses, m = 110-113 gm; driving spring constant $\approx 2 \times 10^4$ dyne/cm; connecting spring constant $\approx 1.6 \times 10^4$ dyne/cm. Connecting springs under an average tension of 1.3×10^5 dynes, driving plate velocity = 0.03 cm/sec.

7. Cohen (1977b)

One dimensional computation model similar to Dieterich's (1972) models a. and d. Spring constants = $10^{16} - 10^{18}$ dynes/cm; $1.5 \leqslant k_2/k_1 \leqslant 5$; $10^2 \leqslant \tau \leqslant 10^4$ sec; $0 < f^s < 3 \times 10^{20}$ dynes; $0 < f^d/f^s < .99$

8. Cohen (1977a)

One dimensional computational models using elastic springs. Spring constants 5×10^{16} dynes/cm - 1.5×10^{17} dynes/cm; $f^s = 1 \times 10^{20}$ dynes - 3×10^{20} dynes; $f^d = 0.8\ f^s$.

9. Rundle and Jackson (1977)

One dimensional computational model employing 20 massless elements driven by moving plate both an elastic and unelastic model are invested.

a. elastic model: driving spring constants = 100–10,000 kbars/cm; connecting spring constant 0–3200 kb/cm; static friction 0.3 kb – 9 kb.

b. anelastic model: The frictional strength is time and stress dependent with

$$\frac{dF^s}{dt} = -\frac{1}{\tau}[\sigma(t) - F^{su}]$$

where $\sigma(t)$ = time dependent stress on the block, and F^{su} and τ are constant.

In the choice of numerical values for the spring constants in the various simulations, little attention has been devoted to the relationship between the driving and connecting spring constants. However, Yamashita (1976) has analzed the relationships between the spring constants and the elasticity constants μ and λ where μ is rigidity and λ the usual Lame parameter. For a one dimensional model he finds

$$k^s = \left[2(\lambda+\mu)\left(\frac{V_s}{V_p}\right)^2 + \mu\right]\frac{\Delta z \Delta x}{\Delta y}$$

and

$$k = \mu\frac{\Delta y}{\Delta t}\Delta x$$

where V_p/V_s is the ratio of primary to secondary seismic wave velocities, and Δz and Δy are the block dimensions along and perpendicular to the fault. The parameter Δz is the dimension of the block in the third direction.

Table I.

Scale factors

length	$a = l/l'$
stress	$b = \sigma/\sigma'$
elastic constants	$c = \mu/\mu' = \lambda/\lambda'$
density	$d = \rho/\rho'$

Scaling relations

force	$F = a^2 b F'$
spring constants	$k = ack'$
displacement	$\Delta x = abc^{-1} \Delta x'$
mass	$m = a^3 dm'$
velocity	$\Delta \dot{x} = b(cd)^{-1/2} \Delta \dot{x}$
acceleration	$\Delta \ddot{x} = b(ad)^{-1} \Delta \ddot{x}$
energy	$E = a^3 b^2 c^{-1} E'$
seismic moment	$M = a^3 b M'$

Scaling laws for source parameters. Source parameters are known in primed system and desired in unprimed system (from Dieterich, 1973).

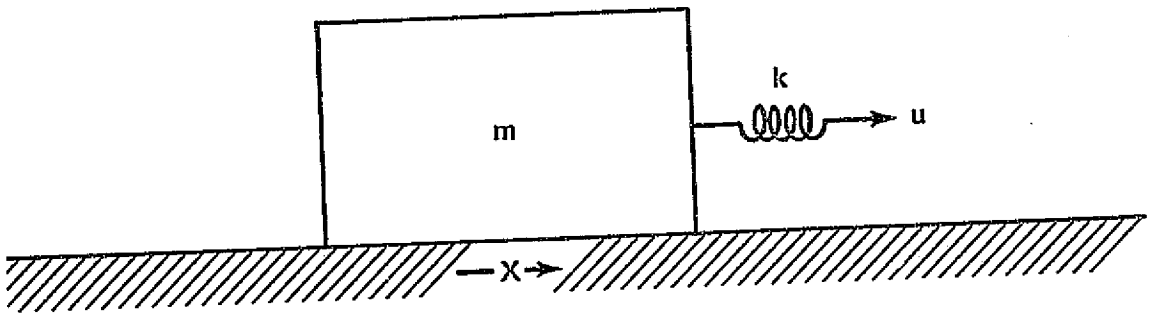

Figure 1: Spring and block model of sliding on a friction surface

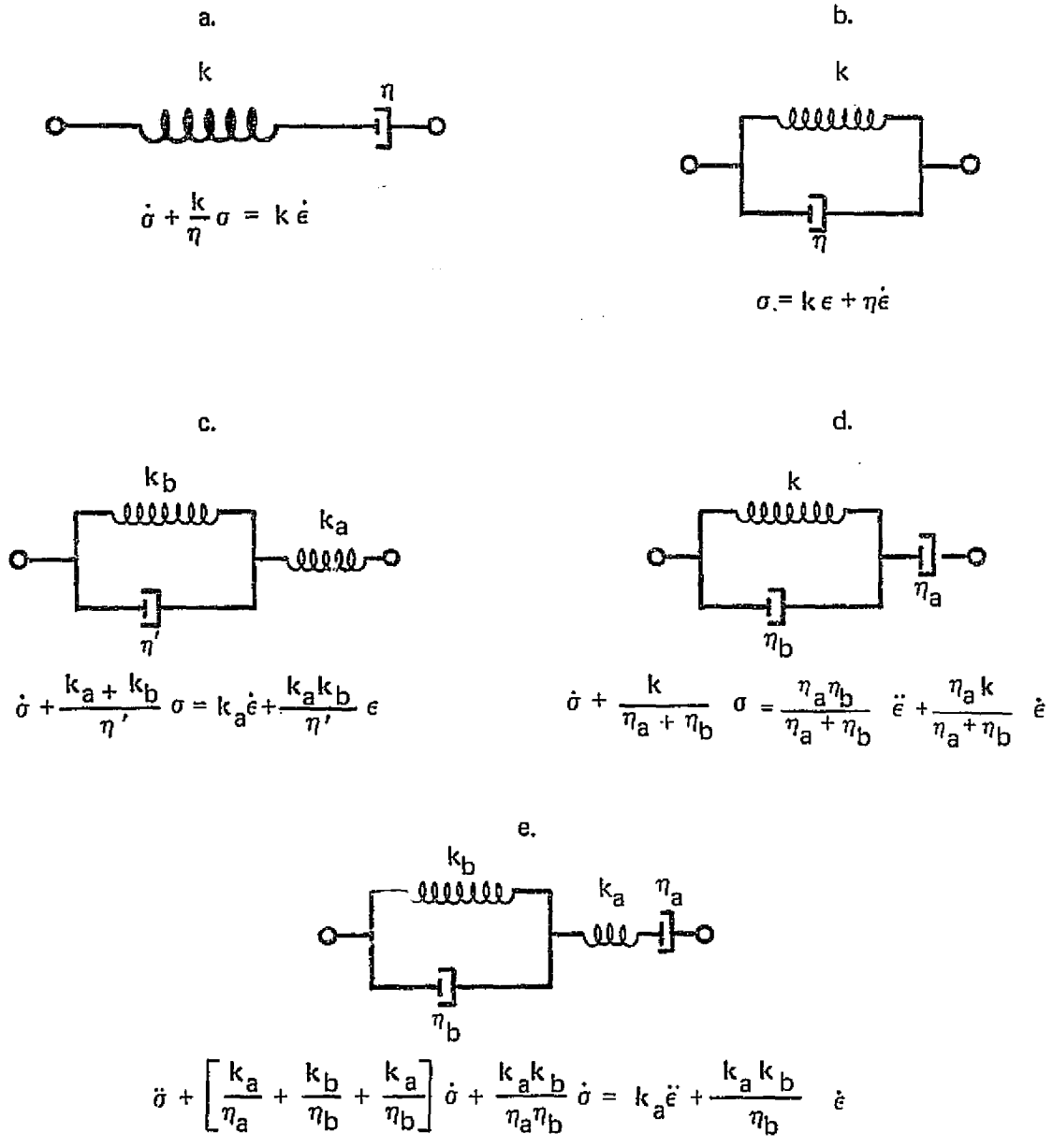

Figure 2. Multiple element rheologic models: a. Maxwell substance, b. Kelvin substance, c. three element generalized Kelvin substance, d. alternative three element substance, e. four element Burgers substance

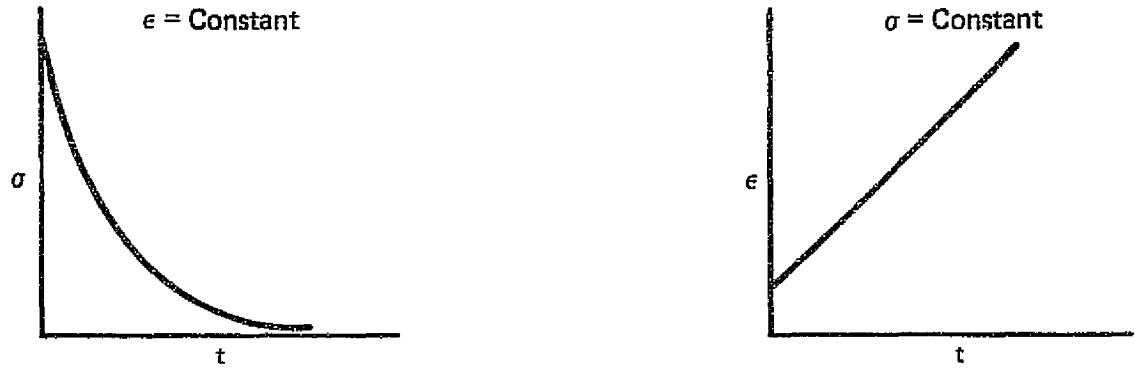

Maxwell substance

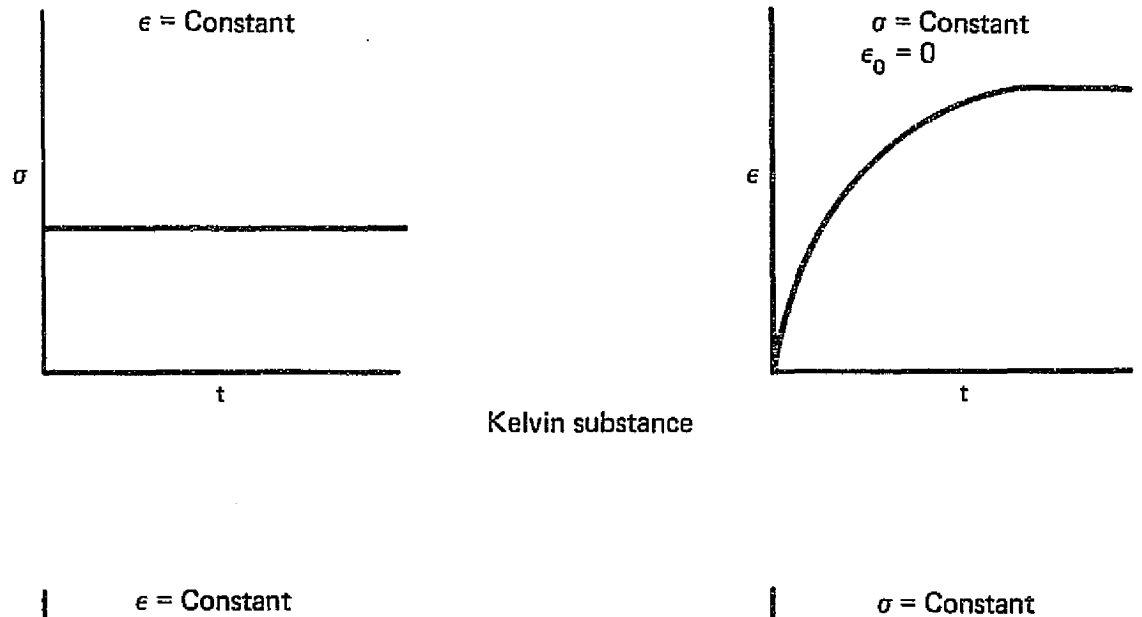

Kelvin substance

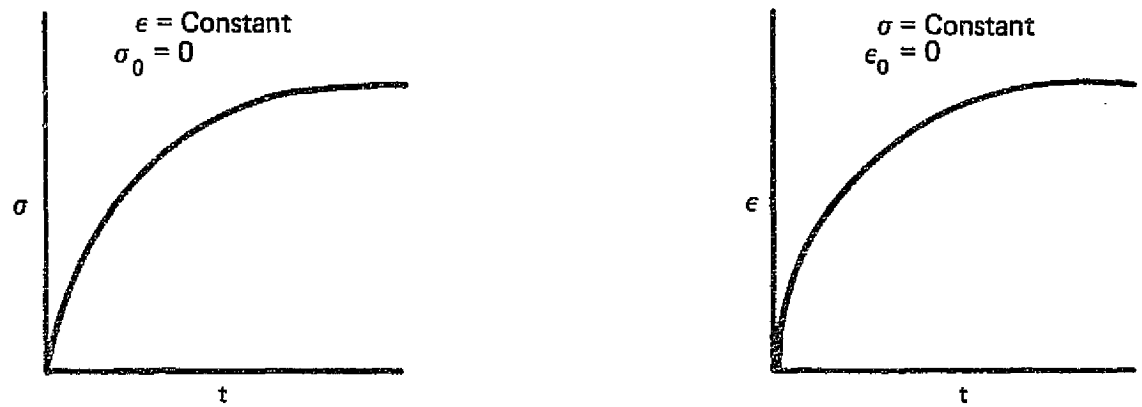

Generalized Kelvin substance

Figure 3: Time dependent behavior of stress and strain for selected linear substances

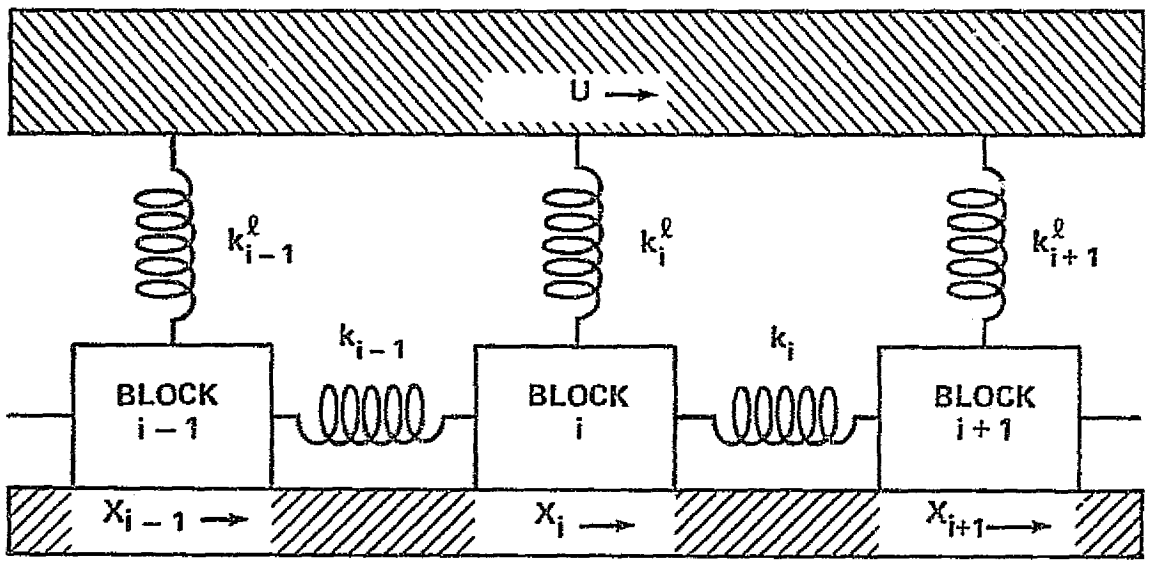

Figure 4: One dimensional fault model

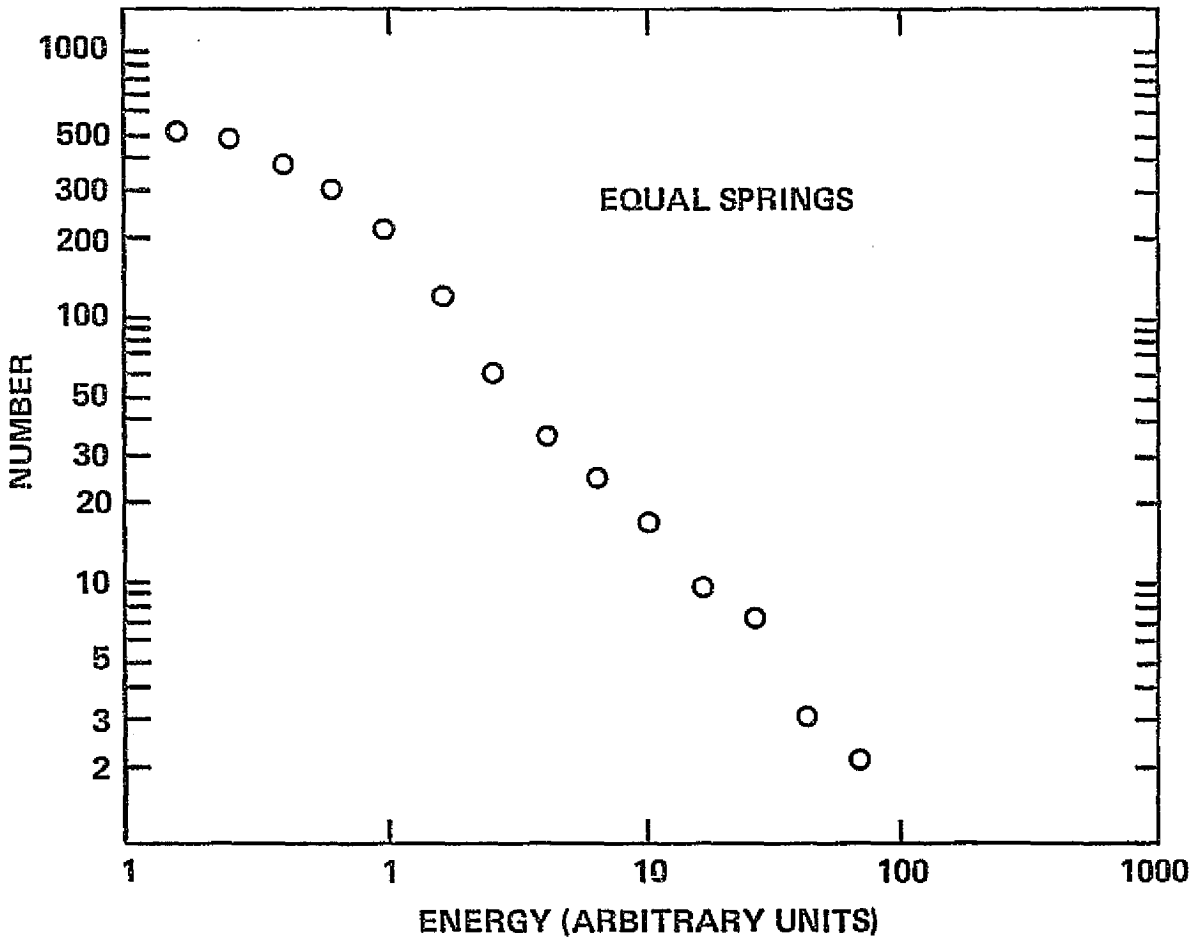

Figure 5: Frequency-energy diagram for mechanical simulator of Burridge and Knopoff (1967)

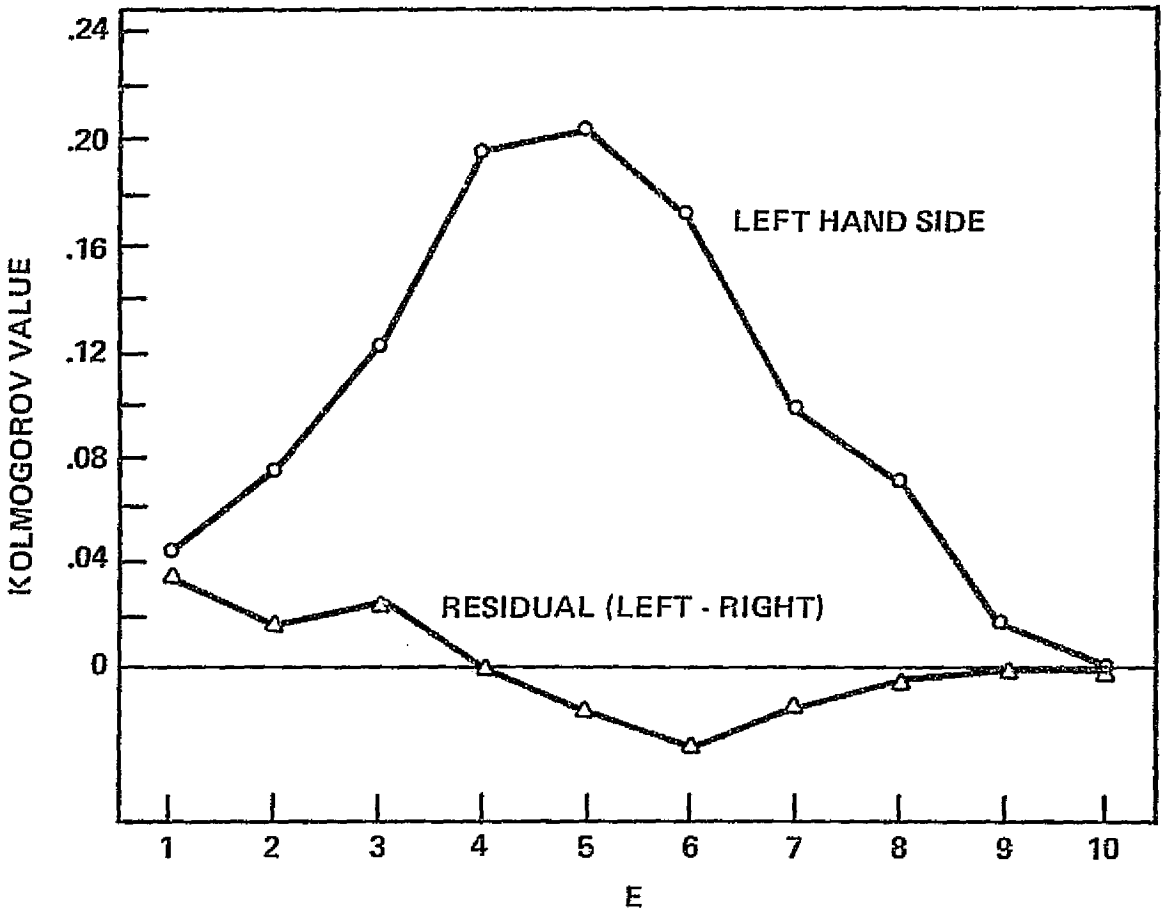

Figure 6: Plot of the values of the Kolmogorov backward equation versus nondimensional energy E, where E has been broken up into 10 energy bands of equal width. The top curve is the left side of the equation and the bottom curve is the residual, defined as the left side minus the right side. (Rundle and Jackson, 1977)

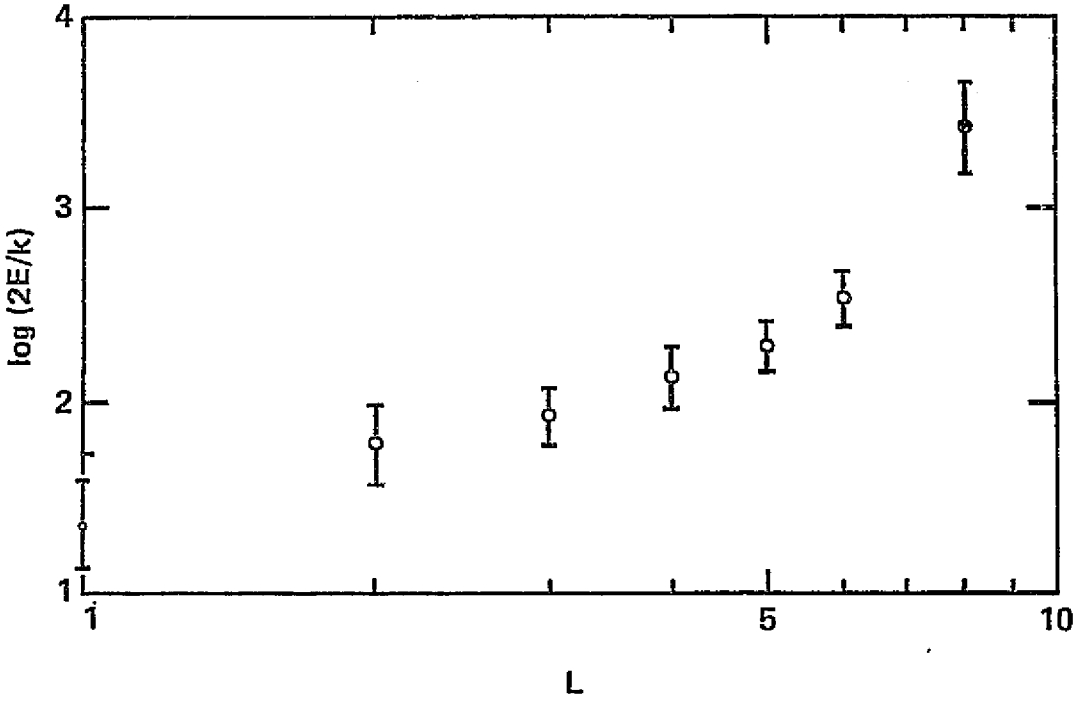

Figure 7: Shock energy versus fault length. Solid dots L = 8; open circles L < 8. (King and Knopoff, 1968(b))

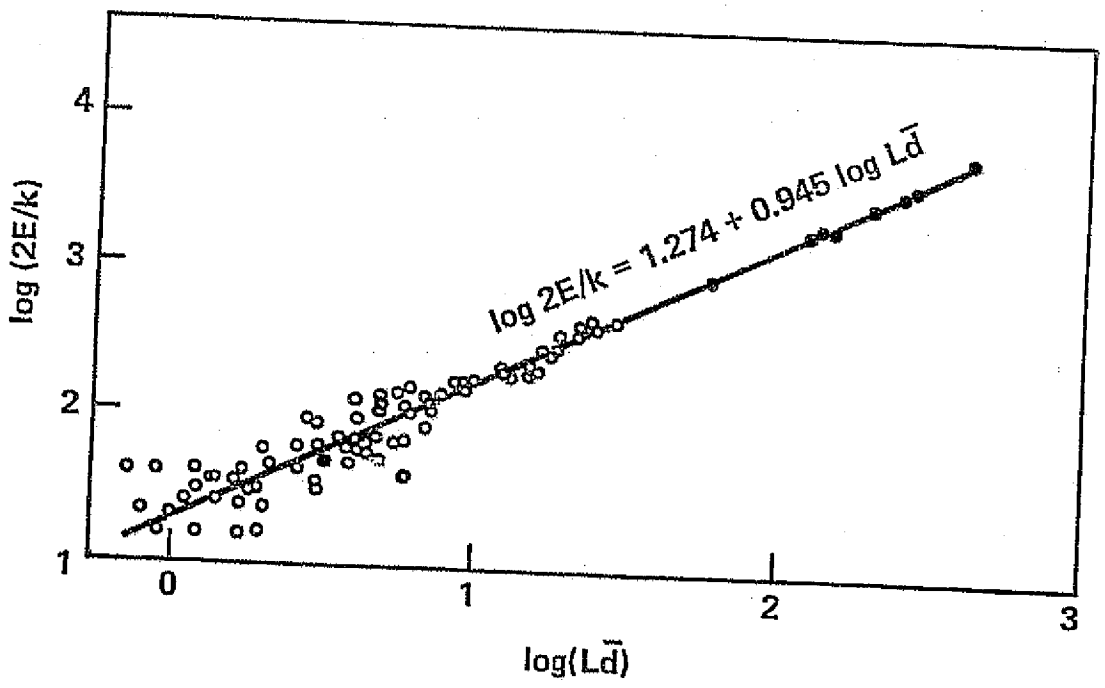

Figure 8: Shock energy versus the product of fault length and average displacement. Solid dots L = 8, open circles L < 8. (King and Knopoff, 1968)

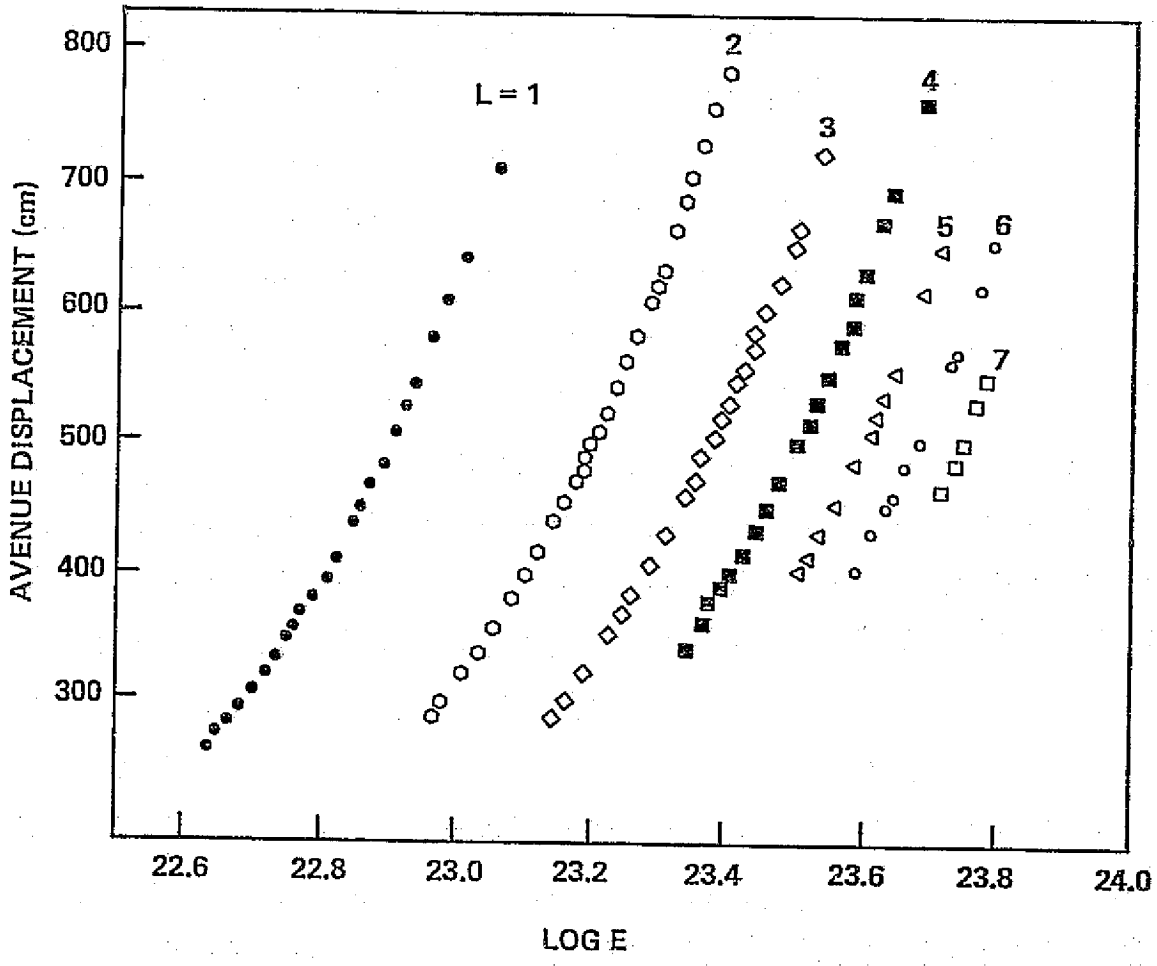

Figure 9: Observed variation in average displacement versus magnitude (log E) for constant friction, varying spring constant simulator (Cohen, 1977a)

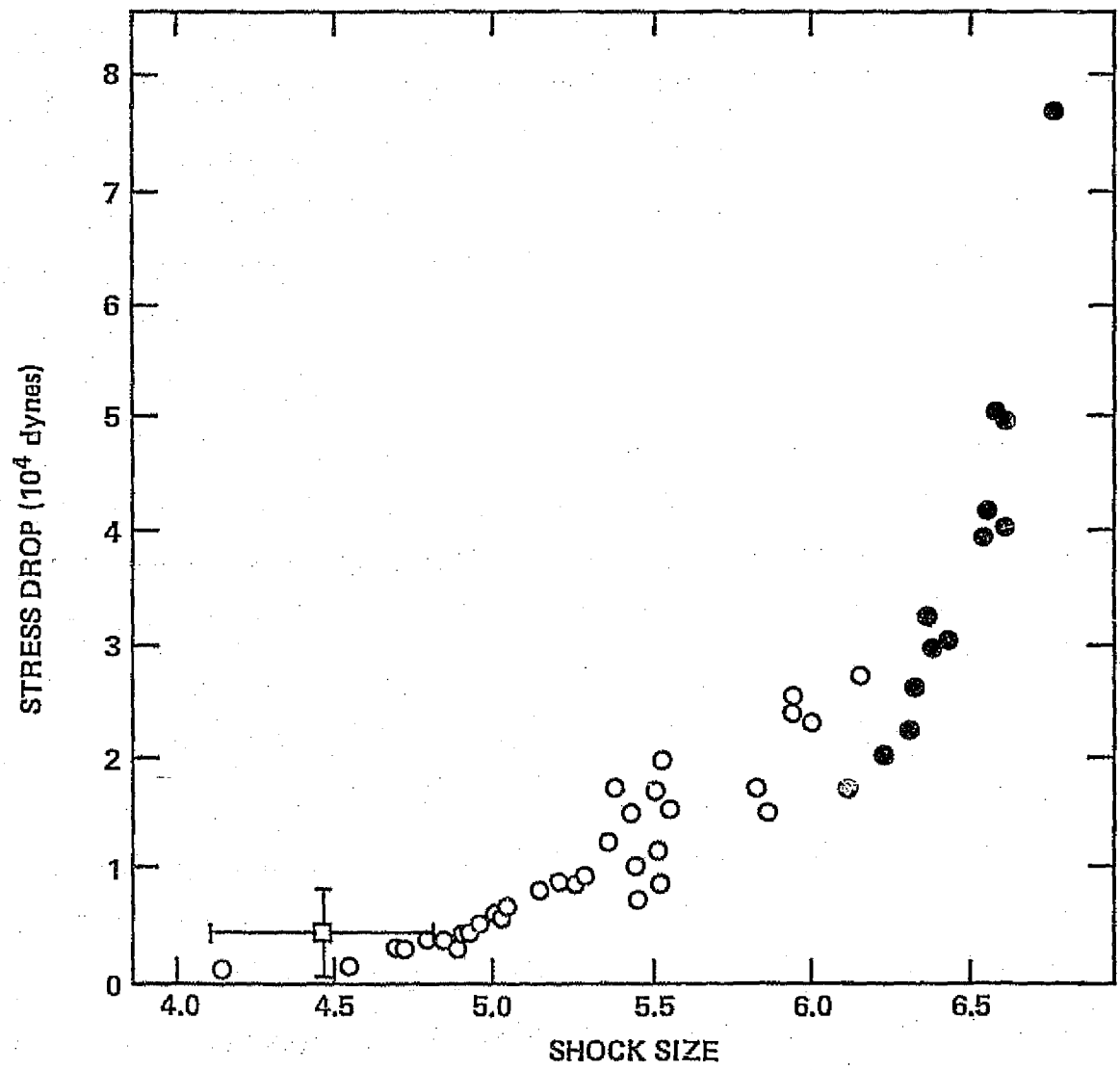

Figure 10: Average drop of stresses in the driving springs versus shock magnitude (log E). Solid dots L = 8; open circles L < 8. (King, 1975)

BIBLIOGRAPHIC DATA SHEET

1. Report No.	2. Government Accession No.	3. Recipient's Catalog No.
TM 78111		

4. Title and Subtitle	5. Report Date
NUMERICAL AND LABORATORY SIMULATION OF FAULT MOTION AND EARTHQUAKE OCCURRENCE	6. Performing Organization Code
7. Author(s)	8. Performing Organization Report No.
Steven C. Cohen	
9. Performing Organization Name and Address	10. Work Unit No.
Goddard Space Flight Center Greenbelt, Maryland 10771	11. Contract or Grant No.
	13. Type of Report and Period Covered
12. Sponsoring Agency Name and Address	Technical Memorandum April 1978
	14. Sponsoring Agency Code

15. Supplementary Notes

16. Abstract

This paper reviews the simulation of earthquake occurrence by numerical and laboratory mechanical block models. Simple linear rheologies are used with elastic forces driving the main events and viscoelastic forces being important for aftershock and creep occurrence. Friction and its dependence on velocity, stress, and displacement also plays a key role in determining how, when, and where fault motion occurs. The discussion of the qualitative behavior of the simulators focuses on the manner in which energy is stored in the system and released by the unstable and stable sliding processes. The numerical results emphasize the statistics of earthquake occurrence and the correlations among source parameters.

17. Key Words (Selected by Author(s))	18. Distribution Statement
earthquakes, simulator, models, elasticity, viscoelasticity	

19. Security Classif. (of this report)	20. Security Classif. (of this page)	21. No. of Pages	22. Price*
U			

*For sale by the National Technical Information Service, Springfield, Virginia 22151.